FL

Image Cover Sheet

CLASSIFICATION	SYSTEM NUMBER
UNCLASSIFIED	145131

TITLE

EXPERIMENTAL AND NUMERICAL DETERMINATION OF THE NONLINEAR OVERALL COLLAPSE OF IMPERFECT PRESSURE HULL COMPARTMENTS

AN: 95-00401

System Number:

Patron Number:

Requester:

Notes:

DSIS Use only:

Deliver to: BA

PAPER NO.24.

EXPERIMENTAL AND NUMERICAL DETERMINATION OF THE NONLINEAR OVERALL COLLAPSE OF IMPERFECT PRESSURE HULL COMPARTMENTS

by T N Bosman and P J Keuning, Ministerie van Defensie,
Directorate of Materiel, Royal Netherlands Navy,
and N G Pegg, Defence Research Establishment Atlantic,
Department of National Defence, Canada

WARSHIP '93

Paper presented at the International Symposium

NAVAL SUBMARINES 4

BOATS, WEAPONS AND SYSTEMS

AT THE HEATHROW PENTA HOTEL

11 12 13 MAY 1993

EXPERIMENTAL AND NUMERICAL DETERMINATION OF THE NONLINEAR OVERALL COLLAPSE OF IMPERFECT PRESSURE HULL COMPARTMENTS

T N Bosman†, N G Pegg‡, P.J. Keuning†
† Ministerie van Defensie, Directorate of Materiel, Royal Netherlands Navy
‡ Defence Research Establishment Atlantic, Department of National Defence, Canada

ABSTRACT

The increased capabilities and availability of nonlinear finite element codes allows their use for design against nonlinear structural collapse of submarine pressure hulls. Analysis can be undertaken on complete structural compartments including the effects of out-of-circularity, secondary structure and residual stresses. As a step towards adopting nonlinear finite element calculations in the design process, a joint Canada/Netherlands Navy project was undertaken to verify calculations of the overall collapse mode of pressure hull failure. A series of machined pressure hull models with enforced out-of-circularities and attached secondary deck structure were constructed, instrumented to measure bending and membrane strains and tested to failure. The strain results were compared to nonlinear finite element and equation-based solutions. This paper presents comparisons of numerical and experimental results on the effects of out-of-circularity on nonlinear overall collapse.

1. INTRODUCTION

Under the auspices of a Canada/Netherlands Navy cooperative program on Surface Ship and Submarine Design Technology, a working group was created to look at several aspects of submarine structures research. One of the items of interest was the effect of geometric imperfections (out-of-circularity, OOC) and secondary structure (decks, tanks, etc.) on buckling collapse loads of pressure hulls. The ability to predict the overall compartment collapse mode of failure was of particular interest. The presence of imperfections and secondary structure can cause the pressure hull to reach yield and collapse at a pressure lower than for a geometrically perfect ring-stiffened cylinder.

The approach used to investigate this problem involved a combination of analytical study and experimental verification. Analytical formulae and nonlinear finite element analyses were used to predict the yield and collapse loads for imperfect ring-stiffened pressure hull compartments. To gain confidence in the numerical predictions of this particularly complex elasto-plastic buckling mode of failure, and possibly to improve prediction methods, a series of physical model tests representing ring-stiffened compartments of submarine pressure hulls with deliberately induced out-of-circularity and internal deck structure were made. This paper describes the experimental and numerical results for three models with out-of-circularity. The secondary structure and combined secondary structure and OOC model results will be reported at a later date.

The 'perfect' models were produced in the Netherlands and shipped to Defence Research Establishment Atlantic, where imperfections were introduced and measured, and the model was instrumented and tested. Section 2 of this paper describes the models and tests. Section 3 describes comparison of experimental and pre-dicted results for the early linear response. The nonlinear behaviour and final collapse comparisons are given in Section 4 and Section 5 gives conclusions to date.

2. MODEL TESTS

2.1 MODEL DIMENSIONS

Three models were created by machining a 520 mm long section of 254 mm diameter, 12.7 mm thick, drawn 6061-T6 aluminum tubing. A photograph and model dimensions are shown in Figure 1. The ring frames were machined into the outside of the tube for ease of manufacture and strain gauge application.

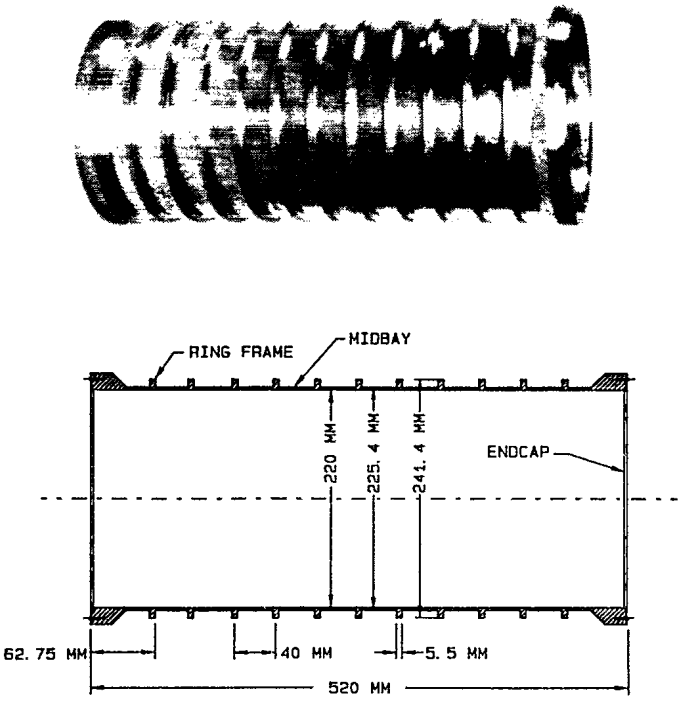

Fig. 1 Photograph of Model and Dimensions

6061-T6 aluminum has a nominal yield stress of 240 MPa. Tests indicated a yield stress between 240 and 260 MPa with a Young's modulus of 71 GPa and Poisson's ratio of 0.32. The plastic modulus (linear strain hardening modulus for a bilinear material model) was found to be 7.0 GPa and the ultimate stress was 270 MPa. These values were used in the nonlinear finite element analysis with ADINA [1] to study this problem. Figure 2 shows the measured stress-strain curve and its bilinear representation used in the ADINA calculations.

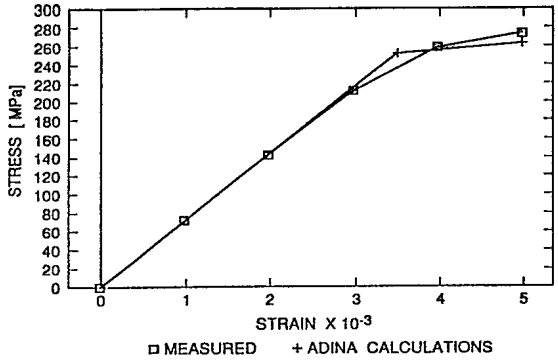

Fig. 2 Stress-Strain Relationship for 6061-T6 Aluminum

6061-T6 aluminum has a higher yield stress to Young's modulus ratio than many materials so that models can be designed which are able to reach elasto-plastic buckling collapse pressures before significant failure through yielding occurs. The models were designed with a ratio of yield to buckling pressure similar to that found in submarine designs. The OOC, expressed as a percentage of hull thickness is also typical of submarines.

2.2 INTRODUCTION OF OUT-OF-CIRCULARITY

The mode of failure investigated with these models was overall buckling collapse initiated by frame yielding. Frame yielding pressures are greatly reduced by out-of-circularity which creates an eccentric load path for the compressive hoop force producing bending moments in the frame. An out-of-circularity in the mode associated with the lowest elastic overall buckling mode of the cylinder is the worst case. In order to control the collapse behaviour, a deliberate out-of-circularity in the overall buckling mode of harmonic n=3 was induced mechanically into the models by a heavy circular frame with three screws spaced at 120 degress. This device applied force to three ring frames at a time.

The cylinder was then measured at 24 circumferential locations on each frame and the out-of-circularity Fourier amplitudes were determined. The results of these are given in Table 1. The maximum deviation from the mean circle for Model 1 was 30 percent of the shell thickness of which the maximum component is in n=3 with an amplitude of 0.44 mm corresponding to 16 percent of the thickness or 0.4 percent of the radius. The maximum deviation from the mean circle for Model 2 was 42 percent of the shell thickness of which the maximum component is in n=3 with an amplitude of 0.68 mm corresponding to 25 percent of the thickness or 0.6 percent of the radius. The maximum deviation from the mean circle for Model 3 was 36 percent of the shell thickness of which the maximum component is n=3 with an amplitude of 0.59 mm corresponding to 22 percent of the thickness or 0.5 percent of the radius. The amplitude of out-of-circularity is maximum in the center ring and reduces towards the cylinder ends.

TABLE 1

Fourier Out-of-Circularity Imperfection Amplitudes (mm) for 'Imperfect' Models

Mode Number	Frame Number (6 is center) 4	5	6	7	8
Model 1					
1	0.0534	0.1172	0.0818	0.0522	0.0402
2	0.0814	0.1551	0.1302	0.1041	0.0806
3	0.2180	0.4289	0.4438*	0.3468	0.1985
4	0.0172	0.0322	0.0317	0.0366	0.0258
5	0.0064	0.0439	0.0316	0.0184	0.0110
6	0.0121	0.1429	0.1592	0.0983	0.0094
7	0.0108	0.0217	0.0368	0.0397	0.0114
8	0.0058	0.0074	0.0053	0.0102	0.0055
Model 2					
1	0.0112	0.0215	0.0278	0.0405	0.0212
2	0.0903	0.0990	0.1029	0.0321	0.0784
3	0.5523	0.6600	0.6755*	0.5664	0.5209
4	0.0270	0.0376	0.0603	0.0345	0.0495
5	0.0104	0.0277	0.0314	0.0330	0.0213
6	0.1438	0.1864	0.1724	0.1017	0.1260
7	0.0081	0.0103	0.0192	0.0167	0.0115
8	0.0059	0.0111	0.0156	0.0334	0.0055
9	0.0644	0.0818	0.0740	0.0336	0.0567
Model 3					
1	0.0056	0.0162	0.0198	0.0354	0.0299
2	0.1952	0.1898	0.1842	0.1678	0.1375
3	0.5111	0.5852	0.5941*	0.5836	0.5455
4	0.0475	0.0597	0.0642	0.0571	0.0385
5	0.0198	0.0237	0.0187	0.0045	0.0037
6	0.0989	0.1099	0.1023	0.1084	0.1237
7	0.0148	0.0202	0.0200	0.0133	0.0138
8	0.0110	0.0086	0.0062	0.0052	0.0030
9	0.0454	0.0503	0.0504	0.0529	0.0596
*maximum value					

2.3 STRAIN GAUGE LOCATIONS

The quantities determined during the test were the collapse pressure and the membrane and bending stress behaviour leading up to and during collapse. The ring-frame yielding should be greatest in the centre frame

as it has the largest out-of-circularity and experiences the largest stress. Gauges measuring strain in the direction of the frame axis (circumferential direction) were placed on the inside and outside of the frame at 18 locations (every 20 degrees). These allowed the assessment of the axial and bending stresses in the frame. Gauges were also placed in the axial direction of the cylinder at every second position on the inside of the frame. Strains were also measured at four circumferential locations in the midbay location in the circumferential and axial directions on the inside and outside of the shell, for a total of 61 strain gauges.

2.4 TEST APPARATUS AND DATA ACQUISITION

DREA's high pressure test facility (Figure 3) consists of a 2.5 metre deep by 1 metre diameter tank capable of pressures up to about 60 MPa. Pressure is increased by pumping water into the tank and is controlled by shutting the pump on and off. A pressure transducer was used to monitor the pressure in the tank. Pressure was increased in increments of 0.7 MPa and held for about 2 minutes. The pressure increment was reduced to 0.35 MPa as the collapse pressure was approached. The pressure dropped by a small amount during the two minute steady period due to a small leak in the tank.

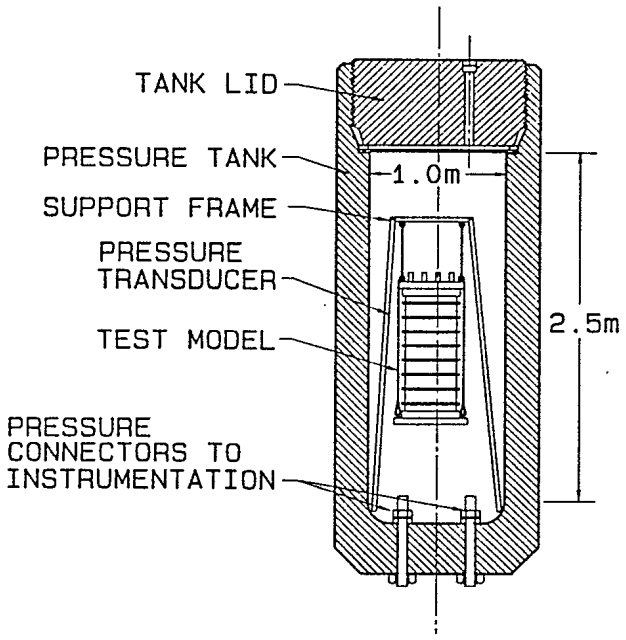

Fig. 3 DREA Pressure Test Facility

Data were recorded by a VAXlab digital acquisition system and stored on optical disks and digital tape.

2.5 EXPERIMENTAL RESULTS

Figure 4 shows the measured circumferential strain versus pressure for the inside and outside of the ring-frame in Model 2. The failure pressures for the three models were 7.14, 6.24 and 6.49 MPa, respectively. Photographs of a collapsed model are shown in Figures 5 and 6.

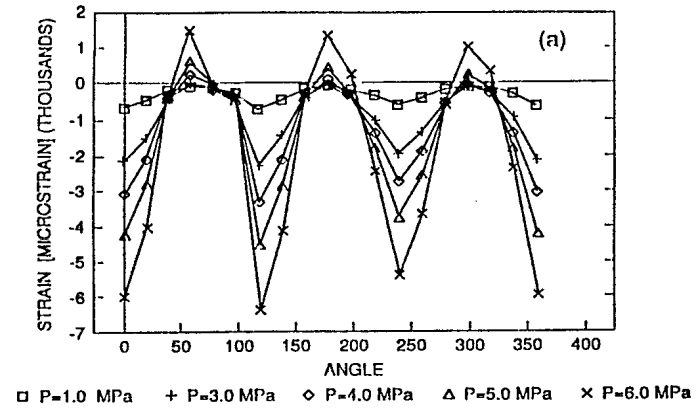

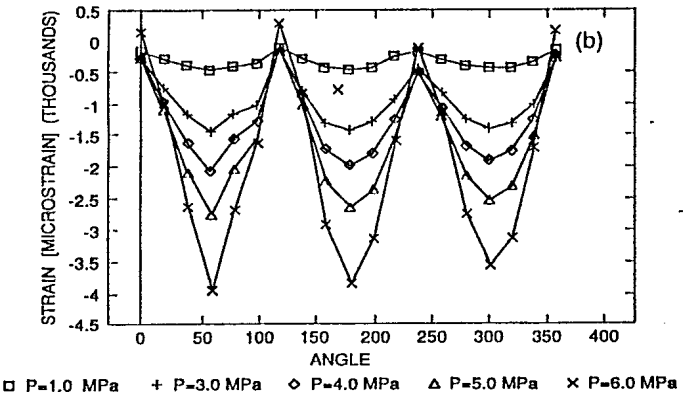

Figs. 4 **(a)** Outside and **(b)** Inside Circumferential Strain on the Stiffening Ring versus Pressure for Model 2

The results for Model 1 were considered less reliable than the other two as problems with leaking in the model were apparent after the test was completed. Modifications to later models prevented this problem.

Additional details of the test procedure can be found in [2].

3. COMPARISON OF LINEAR RESPONSE

Over the early part of the tests, at low pressure levels, the response of the models is linear with respect to the load. Linear axisymmetric and three-dimensional finite element analysis with the code VAST [3] was compared to the mean axisymmetric hoop strain and linear bending strains resulting from the imperfections. The axisymmetric model consisted of 8-node solid axisymmetric elements and the three-dimensional model consisted of 4-node shells and 2-node hermitian beam elements. The measured imper-

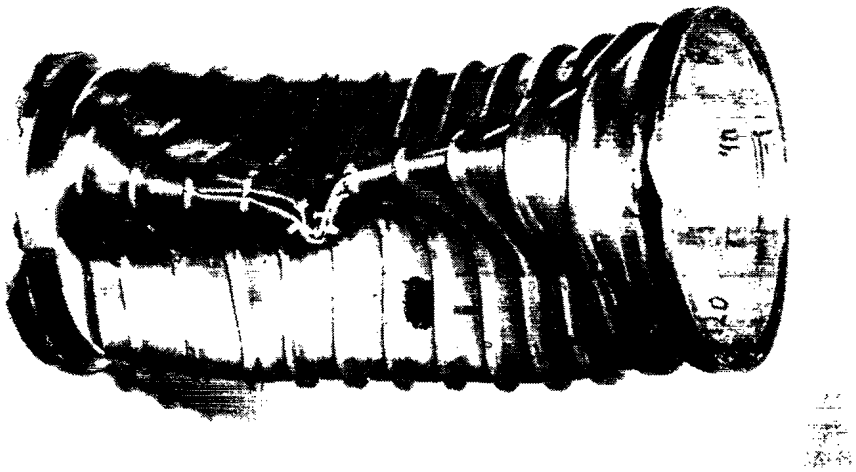

Fig. 5 Photograph of Collapsed Model - Sideview

Fig. 6 Photograph of Collapsed Model - Endview

fections were incorporated in the three-dimensional model. The three-dimensional finite element model with exaggerated imperfections is shown in Figure 7.

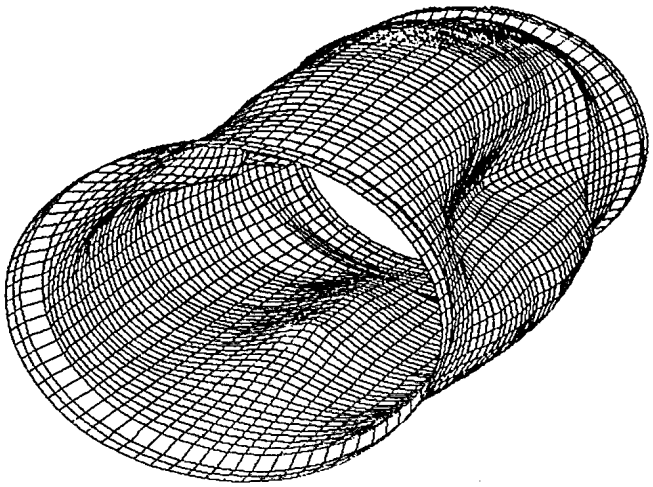

Fig. 7 Finite Element Model with Exaggerated Imperfections (50 X)

Table 2 gives the results of the mean, n=0 (hoop) strains for the axisymmetric and 3-D finite element models, and the three model tests. The strains are a result of a unit (1.0 MPa) pressure load and are derived from the tests by taking the slope of the strain versus pressure curve up to the 1.5 MPa load level. In general, there is good agreement between the two finite element modelling options and the three experimental results for the mean strain values in the linear range.

TABLE 2

Finite Element and Experimental Axisymmetric Strains (με) for Linear Response

Location	Axi FEA	3-D FEA	Model 1	Model 2	Model 3
Inside Ring Circ	-335.6	-318.3	-315.9	-326.3	-337.6
Inside Ring Axial	-313.0	-293.5	-312.8	-252.1	-339.1
Outside Ring Circ	-295.0	-319.6	-280.4	-295.4	-306.6
Inside Midbay Circ	-412.8	-391.3	—	-375.2	—
Inside Midbay Axial	-22.5	-94.0	—	24.3	—
Outside Midbay Circ	-406.7	-391.7	—	—	—
Outside Midbay Axial	-244.3	-282.6	—	—	—
— indicates insufficient data, negative is compression					

The three-dimensional finite element model was also used to compare against linear bending strains resulting from the enforced OOC. Figure 8 shows the comparison between test results and finite element analysis for a unit (1.0 MPa) pressure for the inside and outside ring circumferential strains. The errors between the finite element analysis prediction and three tests were less than 10 percent in the circumferential direction on the inside and outside of the ring frame, but were as high as 25 percent in the axial direction. The errors in the primary Fourier n=3 and 6 components of the inside and outside circumferential strain were less than 5 percent between FEA and experimental values.

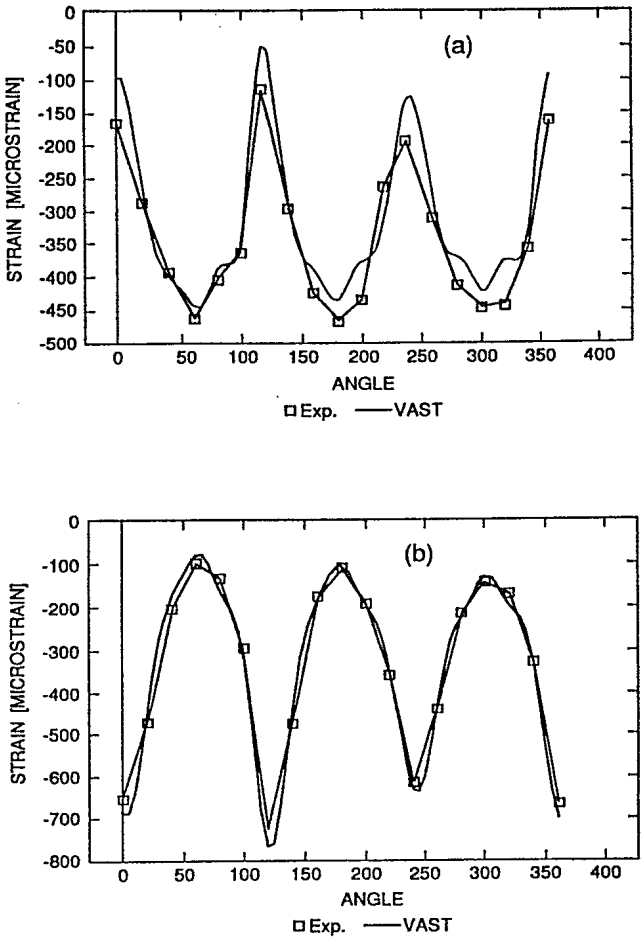

Fig. 8 Comparison of Linear FEA and Test Circumferential Strains at the (a) Inside and (b) Outside Ring-Frame Locations for Model 2

4. COMPARISON OF NONLINEAR RESPONSE

To predict the full collapse history, doubly symmetric, one quarter cylinder finite element models, consisting of 8-node shell and 3-node beam elements, were constructed with ADINA. Using one quarter models introduced some error in the prediction as the imperfections were not truely symmetric in either the cross-sectional or longitudinal planes. The largest imperfections were used in the ADINA models. Table 3 gives the ADINA first yield and collapse predictions versus the experiments for the three models. Further details of the ADINA calculations are given in [5].

TABLE 3

ADINA and Experimental First Yield and Collapse Loads (MPa)

Model	First Yield		Collapse	
	Exp	ADINA	Exp	ADINA
1	5.5	6.0	7.14	7.62
2	4.14	4.10	6.24	6.58
3	4.32	4.63	6.49	6.85

Figure 9 shows the finite element and experimental inside and outside ring circumferential strains at 3.0 and 6.0 MPa for Model 2. At a pressure of 3.0 MPa, the response is still elastic and agreement is very good. At 6.0 Mpa, which is close to the collapse pressure of 6.24 MPa, the differences at the plastic hinge locations are significant, but agreement away from the plastic hinges is still good. The large difference right at the plastic hinge may be due to residual stresses and/or the difference in the measured and modelled stress/strain relationship past yield (see Figure 2).

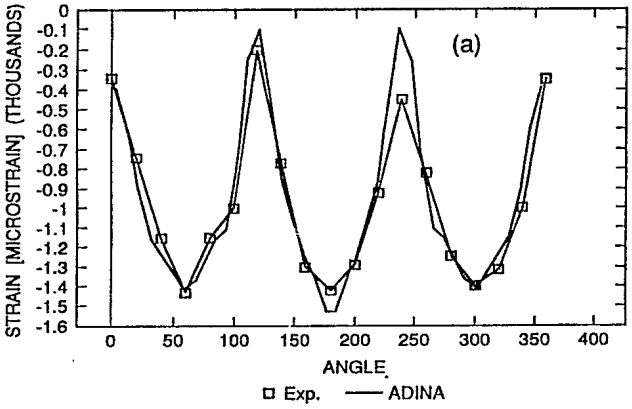

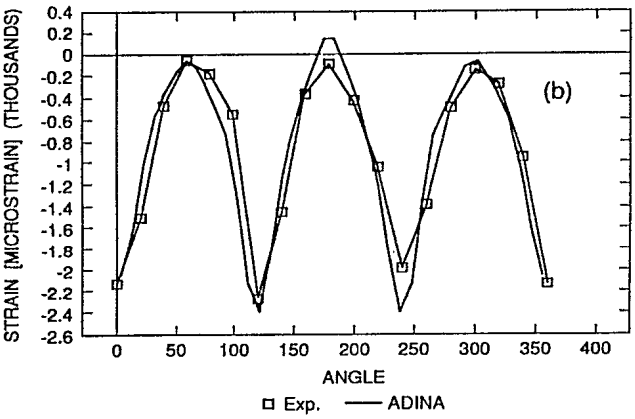

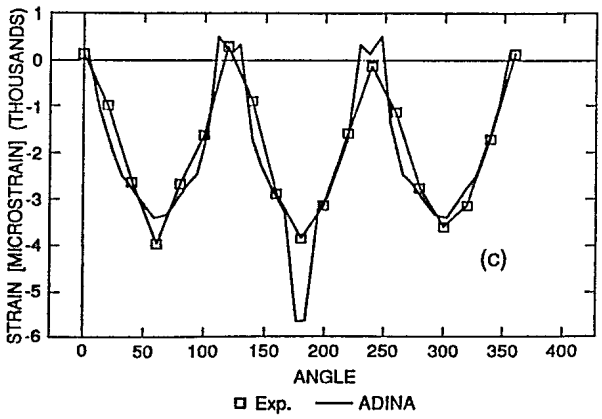

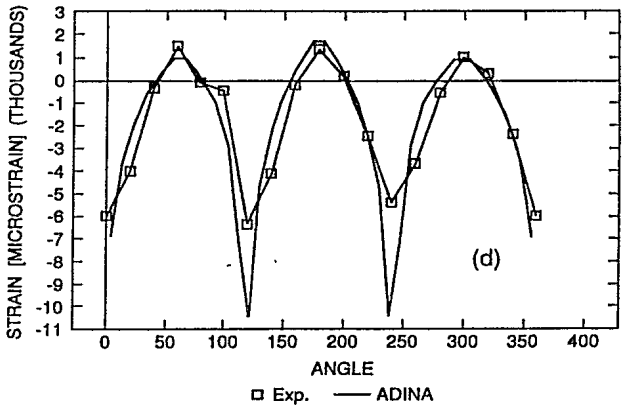

Figs. 9 ADINA and Experimental Strains for Model 2

(a) Inside Ring 3.0 MPa, **(b)** Outside Ring 3.0 MPa,

(c) Inside Ring 6.0 MPa, **(d)** Outside Ring 6.0 MPa

A comparison of the Fourier components of the finite element analysis and measured strains was also made and is shown in Figure 10 for Model 2. Agreement was not quite as good for the other two models where the spread increased near the failure loads.

Figure 10 gives results for Fourier components n=0, 3 and 6 only. Harmonics 2 and 4 were also calculated but are not shown here. Their values were small, in the same order as the n=6 components.

Figure 10 shows that agreement is is very good on the outside of the ring up to 5.0 MPa where local yielding begins. This local yielding has a much larger effect on the n=6 term than the n=0 and 3 terms since it is expected that localized behaviour should have a greater effect on higher order terms.

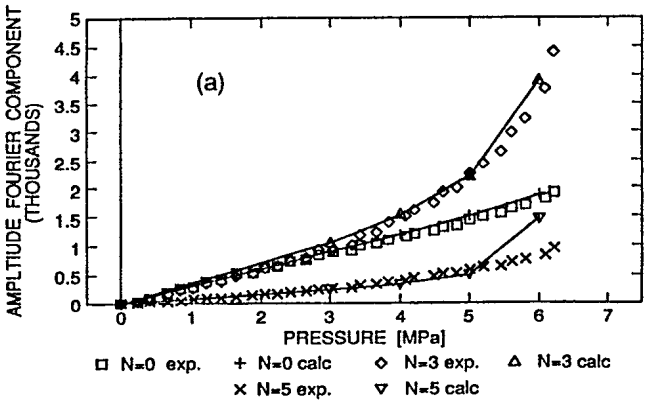

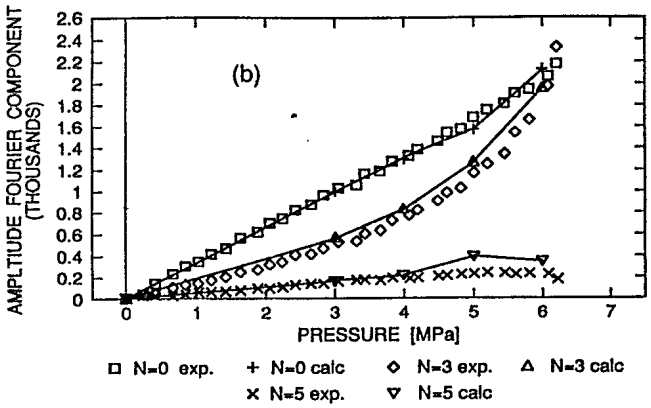

Figs. 10 Fourier Components for the ADINA and Experimental Strains for Model 2

(a) Outside Ring **(b)** Inside Ring

The nonlinear finite element analyses overestimate the first yield pressures to within 10 percent or less and overestimate the collapse pressures to within 7 percent or less. The elasto-plastic collapse load of a perfect model was predicted with BOSOR5 [6] to be 8.3 MPa. The large extent to which OOC reduces the structural capacity of these ring-stiffened pressure hull models is quite obvious from the test and numerical results.

5. OOC VALUES FOR DESIGN

Since it is a well recognized fact that OOC affects the performance of submarine pressure hulls, it is necessary to take this into account in their design and construction. In design, an assummed OOC using a single harmonic shape corresponding to the minimum elastic buckling mode and some specified amplitude is used to determine collapse loads. OOC is measured at various times during construction and compared to build tolerance OOC amplitudes which are required to be less than those used in the design calculations. The experimental study described in this paper allows a comparison between different methods of interpreting the measured OOC and the predicted first yield and collapse values using idealized single harmonic imperfections.

The harmonic shape corresponding to the minimum elastic buckling load for the models in this study was n=3. Figure 11 shows the first yield pressure as a function of amplitude with an idealized imperfection in the n=3 harmonic only, calculated using the analytical formulae derived by Kendrick [4]. The nonlinear collapse pressure as a function of amplitude for an idealized n=3 OOC, calculated using ADINA, is also shown in Figure 11.

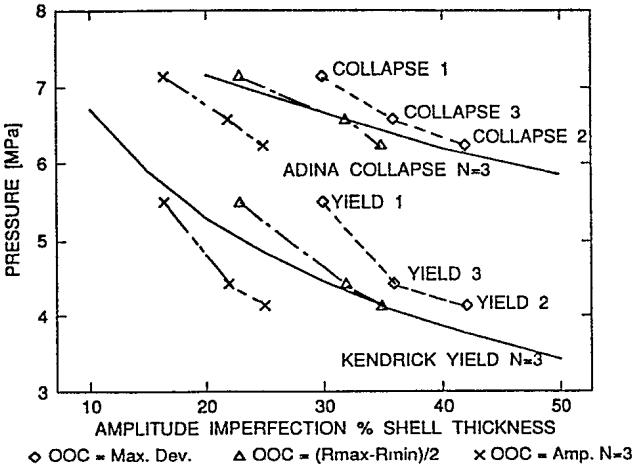

Fig. 11 First Yield and Collapse Comparison as a Function of Methods of Interpreting Measured OOC (MPa)

The OOC in the experimental models was predominantly, but not totally in the n=3 harmonic. The OOC in a real submarine would also have components from several harmonics. The two sets of three experimental curves, one set for each of first yield and collapse, have been derived by plotting the actual collapse and first yield pressures of the model tests against three different ways of representing the measured OOC amplitude. The first method uses the maximum measured deviation from the mean radius, the second method uses half the difference between the maximum and minimum measured radii, and the third uses the n=3 Fourier amplitude only.

For perfect n=3 OOC, the Kendrick formula and ADINA calculation curves underpredict (conservative) the yield and collapse loads for the first method of representing the measured OOC, show good agreement to the second method, and overpredict (unconservative) first yield and collapse in comparison to the third method of representing the measured values. These results suggest that using the second method, of half the difference between the maximum and minimum measured radii to represent a single harmonic amplitude, gives the best results and

could be used for measuring and checking design tolerances. The first method of using the maximum radial deviation appears to always give conservative results.

6. DISCUSSION AND CONCLUSIONS

The purpose of the tests described in this paper was to determine the effect of out-of-circularity on the elasto-plastic strain history and ultimate collapse of ring-stiffened pressure hulls and to verify finite element prediction of elasto-plastic buckling collapse. To this end, imperfections in an n=3 shape were mechanically induced in machined models, accurately measured and incorporated into the finite element analyses.

In general, all three of the test models performed as expected. Failure occurred through initial yielding in the frame which precipitated an overall buckling mode of collapse in an n=3 harmonic shape. The mechanism of failure was elasto-plastic buckling.

Predictions of the strain state in the models through the loading history and overall collapse was done through linear and nonlinear finite element modelling and by the overall collapse equation developed by Kendrick. Predictions of the onset of yield and ultimate collapse were all within 7 percent and the largest error in strain prediction was 25 percent, with most differences being within 10 percent.

Linear finite element modelling was used to predict the axisymmetric (n=0 hoop mode) and bending strains during the early part of the load history. The circumferential membrane and bending strains in the central ring-frame were predicted to within 5 percent of the measured value. Axial strain values were predicted to within 25 percent of the measured values. Errors here likely resulted from residual strains and the effects of imperfections in the shell which were not measured or modelled. The predominant harmonic components of strain in n=0, 3 and 6 were accurately modelled by the linear shell-beam finite element model.

Kendrick's equation [4] for the onset of yield in a ring-stiffened pressure hull compartment was used with two different representations of the measured out-of-circularity. Only a single harmonic component of OOC can be incorporated into this equation, in this case n=3. For the first OOC representation, the total amplitude of imperfection via summing all of the Fourier amplitude components was modelled in the n=3 mode. This is quite conservative and predicts yield to occur at a pressure 6 to 20 percent lower than occurred in the experiments. The second OOC representation used an amplitude in n=3 equal to half of the difference between the maximum and minimum measured radii. This gives smaller OOC values and predictions for this case differed from the measured yield pressure by 0 to 9 percent.

The rectangular frames used in the models have considerable plastic reserve strength and collapse did not occur until significantly after initial yield; collapse loads were as much as 50 percent higher than initial yield loads.

The nonlinear finite element code ADINA was used to predict the behaviour through the entire load history until collapse. The ADINA predictions of first yield were very good with differences of 9, 1 and 3 percent to experimental values for the three models. Predictions of collapse pressure were overestimated by 6.7 percent in the first model and 5.5 percent in the second two models. Comparisons of strain were very good in the linear part of the response with the difference between measured and predicted values increasing as the collapse load was reached; however, predictions were acceptable even in the worst case.

This set of experiments has shown that the prediction methods used give acceptable values for the behaviour of imperfect ring-stiffened cylinder submarine pressure hull sections. Linear finite element calculations gave excellent predictions of the membrane and bending strains at low loads. The Kendrick overall collapse first yield equation and nonlinear finite element calculations predicted the onset of yield in the model within acceptable accuracy. The nonlinear finite element models were able to follow the strain load history and to predict the ultimate elasto-plastic buckling collapse of the models accurately. The effects of out-of-circularity on overall collapse were also clearly demonstrated as collapse loads were as much as 33 percent lower than elasto-plastic collapse loads without any imperfections.

REFERENCES

1. 'ADINA, A Finite Element Program for Automatic Dynamic Incremental Nonlinear Analysis, User's Manual', ADINA Engineering Inc., Watertown, Mass, September 1981.

2. Pegg N.G.,Bosman T.N., Keuning P.J., 'Canada/ Netherlands Experiment on Pressure Hull Collapse - Model 1: Out-of-Circularity Effects', DREA Technical Memorandum, DREA TM/91/212.

3. 'Vibration and Strength Analysis Program (VAST): User's Manual - Version 5', Martec Limited, Halifax, N.S., 1989.

4. Kendrick S., 'Externally Pressurized Vessels', Chapter 9 of The Stress Analysis of Pressure Vessels and Pressure Vessel Components, Ed. S.S. Gill, Permagon Press, 1970.

5. Wallace J.C., Chernuka M.W., 'Finite Element Calculations for Canada/Netherlands Pressure Hull Model Tests', Martec Ltd, Halifax, DREA Contractor Report CR/90/451, November 1990.

6. Bushnell D., 'BOSOR5: A Computer Program for Buckling of Elastic-Plastic Complex Shells of Revolution Including L

227
none

NO. OF COPIES NOMBRE DE COPIES	COPY NO. COPIE N°	INFORMATION SCIENTIST'S INITIALS INITIALES DE L'AGENT D'INFORMATION SCIENTIFIQUE
1	1	CLM
AQUISITION ROUTE FOURNI PAR ▶	DRDRM 7	
DATE ▶		
DSIS ACCESSION NO. NUMÉRO DSIS ▶	95-00413	

DND 1158 (6-87)

National Defence / Défense nationale

PLEASE RETURN THIS DOCUMENT TO THE FOLLOWING ADDRESS:

DIRECTOR
SCIENTIFIC INFORMATION SERVICES
NATIONAL DEFENCE
HEADQUARTERS
OTTAWA, ONT. - CANADA K1A 0K2

PRIÈRE DE RETOURNER CE DOCUMENT À L'ADRESSE SUIVANTE:

DIRECTEUR
SERVICES D'INFORMATION SCIENTIFIQUES
QUARTIER GÉNÉRAL
DE LA DÉFENSE NATIONALE
OTTAWA, ONT. - CANADA K1A 0K2

SYS # 144487

Return to
DRDC CTAL